MANUFACTURING OF TRIPLE-JUNCTION 4 ft² a-Si ALLOY PV MODULES

M. Izu, X. Deng, A. Krisko, K. Whelan, R. Young, H. C. Ovshinsky, K. L. Narasimhan and S. R. Ovshinsky
Energy Conversion Devices, Inc. 1675 West Maple Road, Troy, MI 48084

ABSTRACT

Spectrum splitting, triple-junction a-Si alloy 4 ft² PV modules have been assembled utilizing solar cells produced in a 2 Megawatt continuous roll-to-roll manufacturing line. This manufacturing line produces solar cells on a 5 mill thick, 14 inch wide and 2500 foot long stainless steel roll at a speed of 1 ft/min. The layered structure of the solar cells is: SS/Ag/ZnO/$n_1i_1p_1/n_2i_2p_2/n_3i_3p_3$/TCO, where i_1 is band-gap graded a-SiGe alloy, i_2 and i_3 are a-Si and all of p_1, p_2 and p_3 are μc-Si p^+.

These PV modules provide 9.5% initial and 8.0% stable conversion efficiencies, the highest reported values for a-Si alloy production modules (≥4 ft²).

Major accomplishments which produced the significant efficiency included: 1) the incorporation, for the first time, of a band-gap profiled a-SiGe narrow band-gap solar cell into a continuous roll-to-roll process; 2) the incorporation, for the first time, of a high performance texturized Ag/ZnO back-reflector system into a continuous roll-to-roll process with production subcell yields greater than 99%.

INTRODUCTION

During the past 15 years, Energy Conversion Devices, Inc. (ECD), has significantly advanced the development of materials, device designs, and manufacturing processes required for the commercial acceptance of photovoltaic technology[1-15]. Among these advancements, ECD pioneered and continues development of the low cost, roll-to-roll continuous substrate a-Si alloy thin film solar cell manufacturing process for achieving the cost and efficiency goals necessary for widespread growth of the photovoltaic market.

ECD has recently designed and constructed a 2 Megawatt PV module manufacturing plant for Sovlux, ECD's Russian joint venture company with Kvant. This manufacturing line utilize a continuous roll-to-roll process to produce triple-junction two band-gap solar cells having device configuration which previously demonstrated 13.7% initial efficiency [5]. In this paper, we report the process optimization as well as the progresses and achievements made in this production line.

ECD's a-Si ALLOY PV MANUFACTURING LINE

In ECD's current 2 Megawatt PV Manufacturing line, we deposit a-Si alloy solar cells in a continuous roll-to-roll process on a 5 mill thick, 14 inch wide and 2500 foot long web of stainless steel at a speed of 1 ft/min. Figure 1 illustrates ECD's current manufacturing line.

The front end facility of the manufacturing line

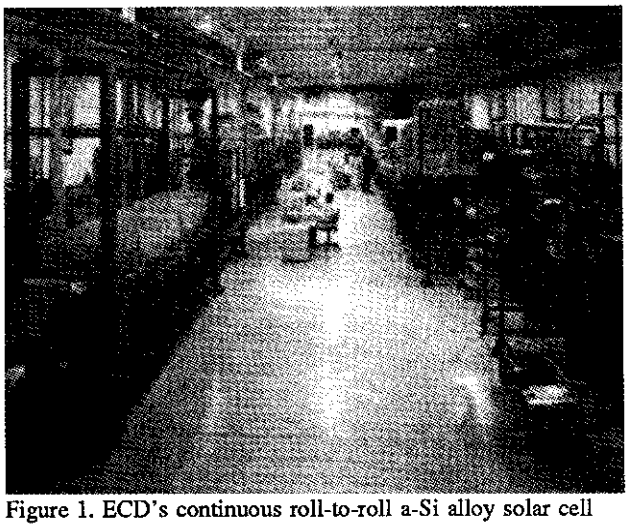

Figure 1. ECD's continuous roll-to-roll a-Si alloy solar cell manufacturing line.

consists of four continuous roll-to-roll machines:

1) A continuous roll-to-roll substrate washing machine that transports the stainless steel web through a ultrasonic detergent cleaning station, multiple deionized water rinsing baths, and an infrared oven drying stage, to produce clean, dry, particle-free substrate suitable for amorphous silicon deposition.

2) A continuous roll-to-roll back-reflector machine that deposits a textured reflective metal layer and a metal oxide layer on the cleaned, stainless steel web as solar cell back-reflector using multiple target DC magnetron sputtering on a heated substrate.

3) A continuous roll-to-roll a-Si alloy RF PECVD deposition machine that produces, in a single pass, sequentially deposited thin films of doped and undoped amorphous silicon alloy semiconductors. This is the key process in a-Si alloy solar cell deposition and will be described in detail later.

4) A continuous roll-to-roll transparent conductor deposition machine that deposits a transparent electrically conductive layer on top of the solar cell structure as an electrical top contact and as an anti-reflective coating using

0-7803-1220-1/93 $3.00

reactive evaporation of metal in an oxygen atmosphere.

The PV module assembly process consists of the following procedures:

1) Slabbing of TCO coated a-Si solar cell rolls into 16" long, 14" wide "slabs".

2) Quality assurance and quality control for performance qualification of production roll.

3)TCO scribing with screen printed etching paste.

4) Short and shunt passivation.

5) Screen printing of Ag paste of grid pattern.

6) Final assembly includes: cell cutting, interconnecting, module laminating, finishing, testing and packaging.

The roll-to-roll continuous manufacturing line for the deposition of a-Si alloy solar cells is designed for a large scale, low cost, uniform and reliable operation. a-Si alloys are produced in a single pass on a 2500 ft. substrate. The operating cost, which includes maintenance and labor, is low.

The 5 mill thick stainless steel substrate is light weight and flexible. It offers many advantages as compared to glass substrates. Stainless steel is breakage free during operation and handling. This thin stainless steel substrate can be heated and cooled quickly during deposition, no waiting time is needed for temperature stabilization. During the deposition, the substrate transport mechanism is simple and reliable, therefore component wear is much less.

a-Si ALLOY TRIPLE-JUNCTION SOLAR CELL DEPOSTION MACHINE

The a-Si alloy solar cell with 13.7% record high conversion efficiency was demonstrated in ECD's R&D lab in 1988 [5]. This solar cell was achieved by using 1) a-Si/a-Si/a-SiGe triple-junction two band-gap cell structure; 2) band gap profiling in bottom a-SiGe cell intrinsic layer; 3) Ag/ZnO high performance back-reflector.

To produce the most efficient a-Si alloy solar cell modules, ECD has constructed a triple-junction solar cell continuous roll-to-roll deposition machine, as illustrated in figure 2. This machine deposits solar cells with a-Si/a-Si/a-SiGe triple-junction two band-gap structure and with profiled a-SiGe band-gap.

The newly constructed a-Si alloy deposition machine consists of a web pay-off chamber section, nine PECVD process chamber sections for the deposition of a triple-junction device structure and a web take-up section. n1, i1 and p1 chambers are adopted for the deposition of the bottom a-SiGe cell; n2, i2 and p2 chambers are adopted for the deposition of the middle a-Si cell; n3, i3 and p3 are adopted for the deposition of the top a-Si cell. Stainless steel web, coated with Ag/ZnO back-reflector from the continuous roll-to-roll sputtering machine, is pulled from the pay-off, through each of the nine deposition chambers, to the take-up chamber. Mixtures of feedstock gases are decomposed at a pressure of approximately 1 Torr in the nine interconnected RF CVD plasma chambers to deposit amorphous silicon alloys continuously on the stainless steel substrate that is heated to approximately 200 C to 300 C. The process gas mixtures in each section are dynamically isolated from adjacent sections

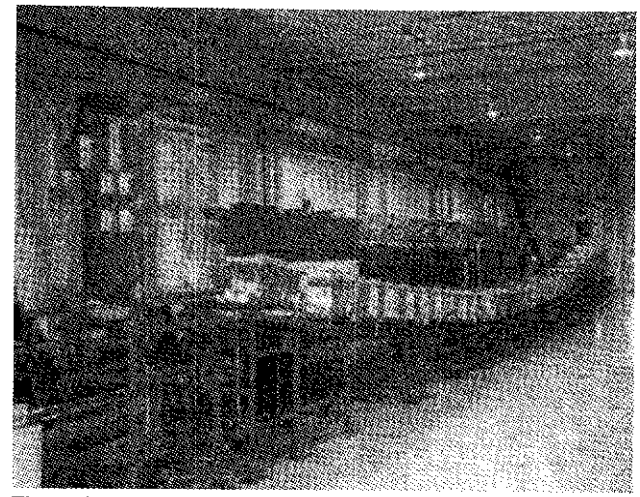

Figure 2. ECD's continuous roll-to-roll a-Si alloy rf PECVD deposition machine.

by proprietary "gas gates." The "gas gates" utilize laminar gas flow through constant geometrical cross section conduits in a direction opposite to the diffusion gradient of the dopant gas concentrations. In this way, migration of dopants between chambers is essentially eliminated and gas mixtures in adjacent chambers are effectively isolated even though no actual physical impediment is present. Substrate transport is accomplished with controlled tension and magnetic rollers for accurate positioning of the substrate in the various process chambers. The web is steered in the take-up chamber to insure that the substrate is properly wound. Substrate passage through the process chambers is such that deposition takes

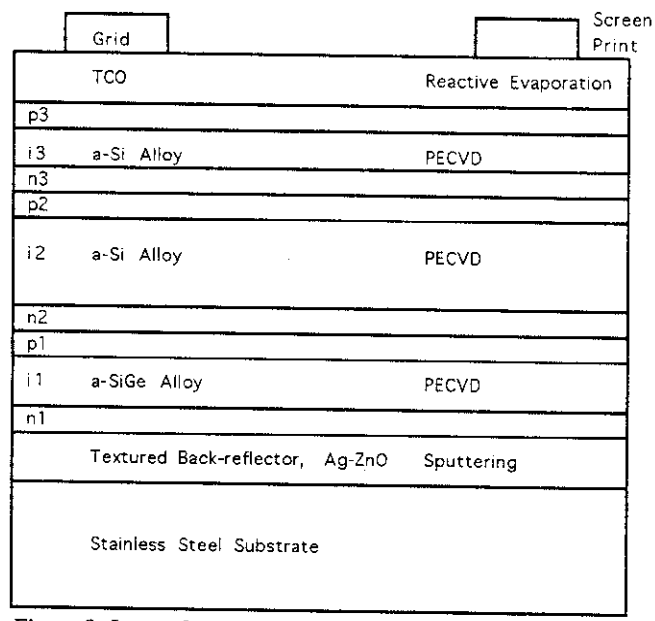

Figure 3. Layered structure of a triple-junction spectrum-splitting solar cell made in ECD's PV manufacturing line

place on the underside, which minimizes film defects due to particulate accumulation. The structure of the solar cell produced in this manufacturing line is illustrated in figure 3.

To achieve band-gap profiling in the continuous roll-to-roll machine, a proprietary gas distribution manifold and cathode configuration were designed and incorporated in the roll-to-roll machine. This gas distribution manifold delivers gas mixtures containing different amounts of GeH_4 into different parts of the i1 chamber. The band-gap profiling is designed such that relatively higher Ge content is on the side of i layer closer to the p^+ layer [14]. With such a profiled band-gap, more light is absorbed near the p^+ junction to minimize the distance holes must travel to get collected. Also, the graded band-gap profiling induces an internal field to aid holes traveling toward the p^+.

PROCESS OPTIMIZATION

During the process optimization of the a-Si alloy deposition machine, we systematically investigated the dependence of sub-cell efficiency on the thickness of each layer and the component cell current matching. We explored the effect of different current mismatching conditions on device efficiency by adjusting the thickness of i1, i2 and i3 layers.

When the i3 layer was thinner, J_{sc} decreased. However, the fill-factor increased because the current limiting thin top cell has a higher fill-factor and also mismatched cells give a higher overall fill-factor. In addition, the top-cell limited devices have better stability because the thinner top-cell is more stable. Therefore, we designed the device to be top-cell limited. Since EVA/Tefzel encapsulation absorbs some light, we produced the top i layer (i3) slightly thicker to compensate the current loss due to EVA/Tefzel absorption and still maintain the proper current matching. The i1 layer was designed to have the highest current since it is the component cell with a relatively low fill-factor.

We also studied and adjusted the deposition conditions of all n^+ a-Si and $p^+\mu c$-Si layers to achieve the following:

* proper doping and thickness to maintain high V_{oc};
* minimum thickness to reduce the absorption. This is especially important for the p3 layer.
* good tunnel junctions between p1 and n2 and between p2 and n3 layers;
* minimized series resistance.

All p layers of the three component cells are $p^+\mu c$-Si. The μc-Si p^+ material absorbs less light and creates higher build-in potential than a-Si p^+. It also reduces the series resistance due to its high conductivity.

Each of the nine layers was optimized under the production condition of 1 ft/min in the continuous roll-to-roll machine shown in Figure 2.

After process optimization, we produced triple-junction solar cells with 11.1% initial active area conversion efficiency. This is the highest efficiency achieved in any a-Si alloy production machine. The J-V characteristics of the solar cell is shown in figure 4. This cell was deposited in a 2500 ft long production run. The ITO and Ag grids were deposited in

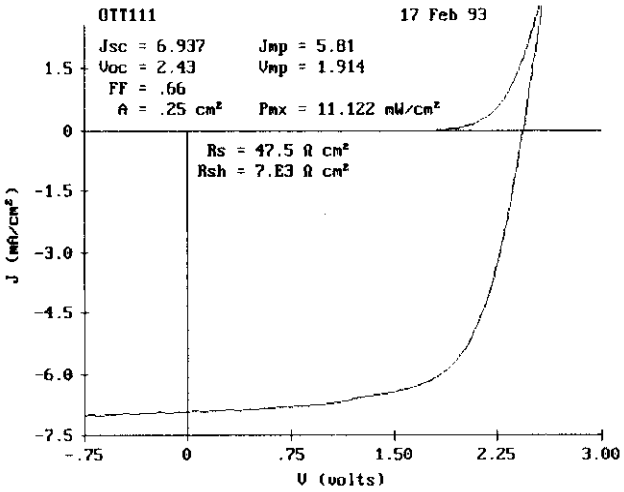

Figure 4. J-V curve of a small area triple-junction solar cell showing 11.1% efficiency. This cell was made in a production run.

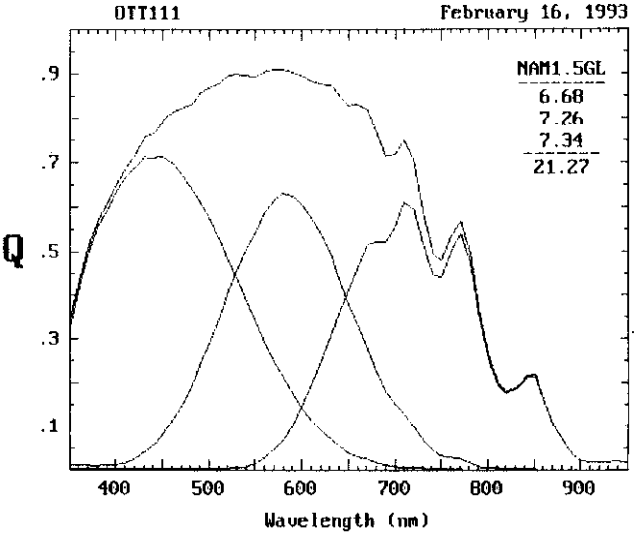

Figure 5. Quantum efficiency curve of a triple-junction solar cell showing 11.1% efficiency.

batch evaporation systems for evaluation. Figure 5 shows the quantum efficiency (QE) curves of this triple-cell showing an excellent response. The QE curve of each component cell was measured in QE system with optical and electrical bias [16]. From the QE curve, we calculated the component cell short circuit current density using AM1.5 global solar spectrum to be 6.68, 7.26 and 7.34 mA/cm² for the top, middle and bottom cell, as shown in figure 5.

QUALITY ANALYSIS

For a PV production line, it is important to have appropriate evaluation of the cell performance through the entire production run, such as cell efficiency, yield, uniformity. In our quality analysis process, statistical samples

Table 1. Cell performance data of 28 cells in a QA/QC sample.

Cell Number	Voc (V)	Jsc (mA/cm2)	FF	Eff. (%)
1	2.38	6.45	0.706	10.49
2	2.38	6.45	0.694	10.64
3	2.37	6.66	0.658	10.37
4	2.37	6.88	0.642	10.46
5	2.37	6.65	0.673	10.59
6	2.38	6.54	0.676	10.52
7	2.38	6.52	0.668	10.36
8	2.39	6.36	0.670	10.19
9	2.38	6.32	0.684	10.29
10	2.37	6.35	0.686	10.30
11	2.37	6.88	0.633	10.31
12	2.37	6.52	0.671	10.36
13	2.38	6.39	0.688	10.45
14	2.39	6.71	0.669	10.72
15	2.38	6.24	0.698	10.36
16	2.38	6.47	0.663	10.20
17	2.37	6.55	0.679	10.54
18	2.37	6.52	0.672	10.39
19	2.37	6.67	0.654	10.33
20	2.38	6.49	0.674	10.40
21	2.39	6.63	0.663	10.50
22	2.38	6.39	0.684	10.39
23	2.37	6.27	0.704	10.47
24	2.37	6.43	0.695	10.59
25	2.37	6.53	0.679	10.50
26	2.37	6.66	0.652	10.30
27	2.38	6.67	0.651	10.34
28	2.38	6.37	0.674	10.21
Average	2.37	6.51	0.673	10.41

Yield for cells with FF>=0.55: 100%

of 4" by 14" were uniformly selected from the production roll. 28 test solar cells of 7.35 cm^2 (7 rows and 4 columns) are processed on each sample by the following procedures: 1) TCO scribing by screen printing of etching paste, heat curing, and rinsing; 2) short and shunt passivation; 3) screen printing of Ag paste grid.

The J-V data of 28 cells in a typical sample, sample 23 of run 109, is summarized in Table 1. The efficiencies of all 28 cells are above 10%. The uniformity is excellent. The average V_{oc}, J_{sc}, fill factor (FF), and efficiency (η) are, 2.37 V, 6.51 mA/cm^2, 0.673, and 10.41%, respectively, as shown in the table. With a subcell yield criterion of FF≥0.55, the subcell yield of this sample is 100%.

To achieve high solar cell efficiency, a high performance textured Ag/ZnO back-reflector was deposited in our continuous roll-to-roll back-reflector sputtering machine, and was used in solar cell production. Despite the high reflectivity of the Ag/ZnO system, the production yield, however, was initially low. Structural, morphological and chemical analysis were conducted at the sites that caused shunts. We have determined that the shorts are caused by defects in the layer structure due to mechanical damage and foreign materials incorporated in the deposited layer during processing. We incorporated several new designs for the production machine to improve the back-reflector by reducing the mechanical damage such as dimples and scratches, as well as eliminating the foreign materials falling on the deposition surface. With these improvements, we effectively reduced the creation of shorts and shunts, and obtained high production yield for the high performance Ag/ZnO back-reflector system. For a 2500 ft. production run we achieved average subcell

Table 2. Average cell performance data of samples throughout an entire production run.

Sample Number	Meter Mark (m)	Voc (V)	Jsc (mA/cm2)	FF	Eff. (%)	Yield (%)
1	41	2.35	6.52	0.661	10.15	100
2	62	2.35	6.64	0.658	10.29	100
3	62	2.36	6.53	0.670	10.35	100
4	82	2.35	6.61	0.655	10.20	100
5	103	2.35	6.55	0.655	10.12	100
6	124	2.35	6.43	0.666	10.08	100
7	166	2.35	6.51	0.659	10.10	100
8	166	2.36	6.54	0.669	10.37	100
9	187	2.35	6.55	0.659	10.16	100
10	208	2.38	6.47	0.654	10.07	96
11	229	2.36	6.49	0.662	10.14	96
12	250	2.36	6.33	0.666	9.97	100
13	271	2.36	6.46	0.667	10.20	96
14	271	2.37	6.41	0.671	10.19	100
15	292	2.39	6.40	0.661	10.14	100
16	312	2.36	6.59	0.658	10.25	100
17	334	2.35	6.56	0.662	10.24	100
18	354	2.35	6.42	0.664	10.05	100
19	375	2.35	6.54	0.662	10.22	100
20	375	2.37	6.48	0.669	10.29	100
21	396	2.37	6.54	0.667	10.36	100
22	396	2.37	6.45	0.676	10.36	100
23	417	2.37	6.51	0.673	10.41	100
24	417	2.37	6.56	0.671	10.45	100
25	438	2.37	6.44	0.667	10.20	100
26	438	2.37	6.52	0.665	10.29	100
27	459	2.37	6.39	0.680	10.33	100
28	459	2.37	6.43	0.671	10.26	100
29	480	2.37	6.46	0.675	10.36	100
30	480	2.37	6.45	0.673	10.31	100
31	501	2.37	6.43	0.674	10.30	100
32	501	2.37	6.47	0.667	10.25	100
33	522	2.37	6.32	0.680	10.23	100
34	522	2.37	6.45	0.671	10.26	100
35	543	2.37	6.39	0.680	10.34	100
36	543	2.37	6.48	0.670	10.32	100
37	564	2.38	6.34	0.670	10.15	100
38	564	2.38	6.32	0.669	10.10	100
39	585	2.38	6.35	0.674	10.20	100
40	585	2.38	6.29	0.679	10.19	100
41	595	2.38	6.32	0.671	10.12	100
42	595	2.38	6.40	0.673	10.29	100
Average		2.366	6.46	0.668	10.21	99.7
Std. Deviation		0.002	0.01	0.001	0.02	0.2

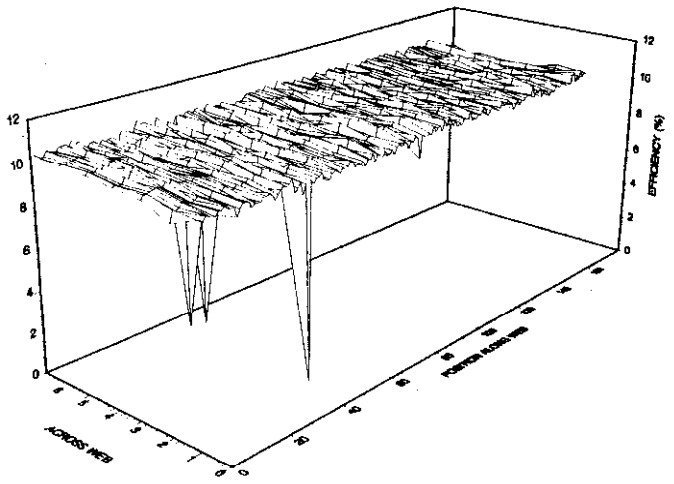

Figure 6. Three dimensional plot of cell efficiency of test cells in a production run.

yield of 99.7%. This is the highest production subcell yield ever achieved in a Ag/ZnO back-reflector system.

In Table 2, we list the averages of V_{oc}, J_{sc}, FF and η, and yield for each of the 42 samples periodically taken from a production run, run#109. The averages from table 1 for sample 23 is also listed in the table for meter mark 417. The average subcell efficiency for the whole production run was 10.21 0.02%. The average subcell yield was 99.7%

Figure 6 is a three dimensional plot of cell efficiency for every cell in this production run. There are 7 cells for each column and 4 42 cells for each row. Out of the 1176 cells, only three failed. As we see from the figure, the solar cell performance is highly uniform throughout the entire run. The results represent the excellent consistency and uniformity achieved in an continuous roll-to-roll manufacturing process.

4 ft² PV MODULES

Strip cells are produced by processing slabs of solar cell material through TCO scribing, short and shunt passivation and screen printing of Ag paste grid pattern. A strip cell is a single solar cell with an aperture of 12.5" x 5.4". After cutting, trimming and bus bar installing, nine strip cells are connected together in series, as a module. A diode is connected in parallel with every strip to prevent the strip cell from being reverse biased. The module is then vacuum laminated, in a high temperature oven, with Tefzel, EVA and crane glass as the transparent front cover. An aluminum frame and junction box are installed to finish the module. Figure 7

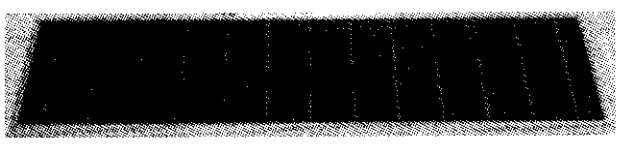

Figure 7. A photographic picture of a 1 ft by 4 ft finished PV module.

is a picture of ECD's 1 ft by 4 ft a-Si alloy production PV module.

To further improve the module efficiency, we investigated the losses from the module fabrication and assembly process. The loss in module efficiency is due to the following three factors: 1) coverage losses due to TCO etching line, grid line, and bus bars; 2) electrical losses due to the resistivity of the TCO, grids and bus bars; 3) current loss due to encapsulation.

We quantitatively investigated the losses by computer modeling, which calculates the dependence of total losses (coverage and electrical losses) on the width of TCO etching line, width of grid line and diameter of the copper wire bus bars based on the known information of the resistivities of TCO, grid line and copper wire as well as the approximate operation characteristics of the module. A new artwork of etching line, grid and bus bar pattern was designed to minimize the efficiency losses to about 13%.

4 ft² triple-junction PV modules were assembled with the improved module design using solar cells produced in our continuous roll-to-roll manufacturing line. Table 3 list the module performance data, of ECD's 4 ft² modules produced over the past 9 monthes, measured at ECD and National

Table 3. Module performance data, of ECD's 4 ft² a-Si alloy solar cell modules, measured at ECD and National Renewable Energy Laboratory.

Module Number	Date Produced	Voc (V)	Isc (mA/cm2)	FF	Pmax (W)	Area (cm2)	Efficiency (%)	Measurement Lab
#01	Jul.92	21.75	2.51	0.59	32.39	3991	8.12	ECD
		21.83	2.525	0.596	32.84	3984	8.24	NREL
#12	Sep.92	21.76	2.59	0.6	33.81	3991	8.47	ECD
		21.79	2.61	0.602	34.21	3997	8.56	NREL
#16	Nov.92	21.27	2.57	0.62	33.93	3945	8.6	ECD
		21.49	2.72	0.592	34.61	3949	8.76	NREL
#23	Mar.93	21.62	2.68	0.628	36.39	3907	9.31	ECD
		21.56	2.72	0.63	36.96	3906	9.46	NREL
#27	Mar.93	21.6	2.72	0.632	37.18	3923	9.48	ECD
#28	Mar.93	21.3	2.75	0.634	37.15	3923	9.47	ECD
#30	Mar.93	21.61	2.68	0.63	36.57	3907	9.36	ECD
		21.51	2.74	0.627	37.01	3906	9.47	NREL

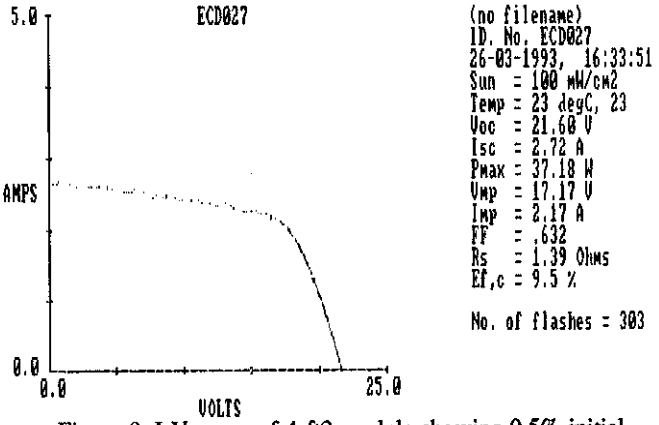

Figure 8. I-V curve of 4 ft2 module showing 9.5% initial aperture area module efficiency.

Table 4. Light soaking test data of two 4 ft² triple-junction PV modules (module 27 and 28). Aperture area=3923 cm².

Module Number	Light Soaking Time (Hrs)	Voc (V)	Isc (A)	Fill Factor	Pmax (W)	Eff. (%)	Drop in Eff. (%)
#028	Initial	21.30	2.75	0.634	37.15	9.5	
	72	20.94	2.67	0.580	32.37	8.3	13
	230	21.05	2.64	0.571	31.72	8.1	15
	393	20.97	2.63	0.573	31.58	8.1	15
	625	20.99	2.62	0.570	31.38	8.0	16
#027	Initial	21.60	2.72	0.632	37.18	9.5	
	40	21.12	2.66	0.579	32.53	8.3	13
	202	20.99	2.63	0.575	31.71	8.1	15
	434	21.02	2.62	0.571	31.47	8.0	15
	600	21.05	2.62	0.566	31.24	8.0	16

Renewable Energy Laboratory (NREL). We have achieved an initial aperture module efficiency of 9.5% and an total power output of 37.2 W for a module of 3923 cm² aperture area. This efficiency is higher than any reported efficiency for a-Si alloy production modules. Figure 8 is the I-V curve of a 4 ft² module measured with a Spire solar simulator, showing 9.5% efficiency.

To measure the stable efficiency of our modules, we conducted light soaking stability tests. Table 5 summarizes the module performance after different light soaking time for two modules, Module 27 and Module 28. Module 27 has been degraded for 600 hours. The stable module efficiency after 600 hours of one sun light soaking at approximately 50 to 60 ℃ under load is 8%, as shown in Figure 9. Figure 10 is the semilog plot of module efficiency of the two modules as a function of light soaking time. Clearly, the module efficiency has saturated.

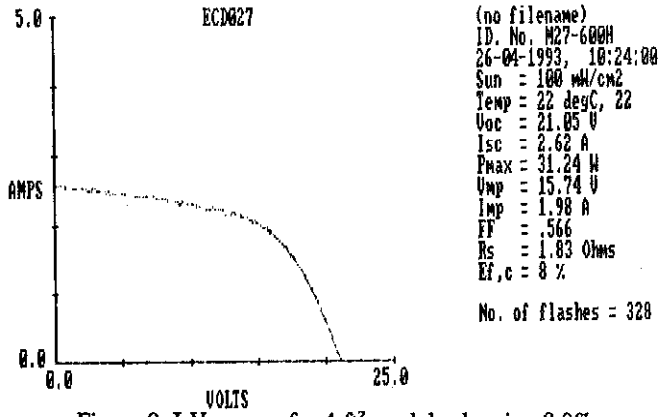

Figure 9. I-V curve of a 4 ft² module showing 8.0% stable module efficiency.

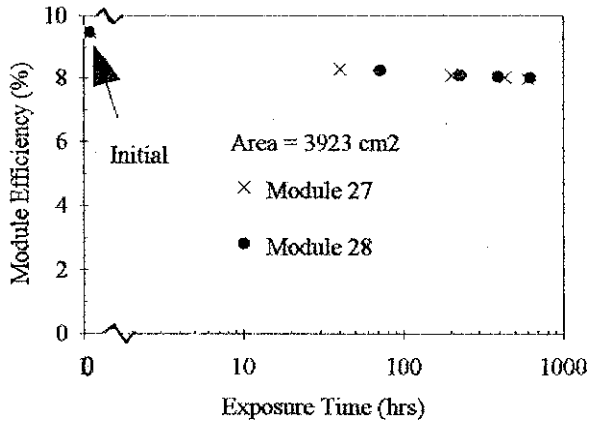

Figure 10. Module efficiencies of two 4 ft² modules as a function of light soaking time under one sun illumination.

SUMMARY

ECD has constructed a 2 Megawatt manufacturing line that produces triple-junction spectrum-splitting a-Si alloy solar cells in a continuous roll-to-roll process. This production line has successfully incorporated:

*Band-gap profiled a-SiGe narrow band-gap solar ce ll deposition in continuous roll-to-roll process using a proprietary gas distribution manifold and cathode splitting configuration;

*Textured Ag/ZnO back-reflector deposition in a continuous roll-to-roll sputtering machine with production subcell yields greater than 99%.

By optimizing the continuous roll-to-roll solar cell deposition process and using the improved module design in the assembly, we achieved:

*Initial active area subcell efficiency of 11.1% in small area triple-junction two band-gap a-Si alloy solar cells produced in a 2 Megawatt continuous roll-to-roll a-Si alloy solar cell deposition machine on Ag/ZnO back-reflector;

*Initial aperture area module efficiency of 9.5% in 4 ft² triple-junction a-Si alloy PV production modules;

*Stable aperture area module efficiency of 8.0% in 4 ft² triple-junction a-Si alloy PV production modules;

*A subcell yield of 99.7% in a 2500 ft long production run.

ACKNOWLEDGEMENTS

The authors would like to thank Dr. Subhendu Guha, Dr. JeffYang and Dr. Hellmut Fritzsche for their helpful discussions and supports. The authors would also like to thank other ECD's project members who contributed to this program. This work was supported by DOE/NREL PVMaT-2A program under subcontract number ZM-2-1104-7.

REFERENCES

[1] M. Izu and S. R. Ovshinsky, SPIE Proc. 407, 42 (1983).
[2] M. Izu and S. R. Ovshinsky, Thin Solid Films 119 55 (1984).

[3] H. Morimoto and M. Izu, JARECT 16 (1984); Amorphous Semiconductor Technology & Devices, North Holland Publishing Company, Edited by Y. Hamakawa, 212 (1984).
[4] S. R. Ovshinsky, Proc. International PVSEC-1, 577 (1984).
[5] J. Yang, R. Ross, T. Glatfelter, R. Mohr, G. Hammond, C. Bernotaitis, E. Chen, J. Burdick, M. Hopson and S. Guha, Proc. 20th IEEE P.V. Spec. Conf. 241 (1988).
[6] J. Yang, R. Ross, R. Mohr and J. P. Fournier, Proc. MRS Symp. Vol. 95, 517 (1987).
[7] P. Nath and M. Izu, Proc. of the 18th IEEE Photovoltaic Specialists Conf., Las Vegas, Nevada, 939 (1985).
[8] P. Nath, K. Hoffman, J. Call, C. Vogeli, M. Izu and S. R. Ovshinsky, Proc. of the 3rd International Photovoltaic Science and Engineering Conf., Tokyo, Japan, 395 (1987).
[9] P. Nath, K. Hoffman, C. Vogeli and S. R. Ovshinsky, Appl. Phys. Lett. 53 (11), 986 (1988).
[10] P. Nath, K. Hoffman, J. Call, G. Didio, C. Vogeli and S. R. Ovshinsky, Proc. 20th IEEE P.V. Spec. Conf., 293 (1988).
[11] P. Nath, K. Hoffman, C. Vogeli, K. Whelan and S. R. Ovshinsky, Proc. 20th IEEE P.V. Spec. Conf., 1315 (1988).
[12] P. Nath, K. Hoffman and S. R. Ovshinsky, 4th International P.V. Science and Engineering Conf., Sydney, Australia, (1989).
[13] S. Guha, A Paper Presented at MRS Spring Meeting, San Diego, April (1989).
[14] J. Yang, R. Ross, T. Glatfelter, R. Mohr and S. Guha, MRS Symposium Proc. Vol. 149, 435 (1989).
[15] S. R. Ovshinsky, M. Izu, H. C. Ovshinsky, Proceedings of World Renewable Energy Congress, in Reading, United Kindom, September 17, 1992.
[16] J. Burdick and T. Glatfelter, Solar Cells, 18, p301 (1986).